A Continuous-Flow System for Asymmetric Hydrogenation Using Supported Chiral Catalysts

József Madarász[1], Gergely Farkas[1], Szabolcs Balogh[1], Áron Szöllősy[2], József Kovács[1], Ferenc Darvas[3], László Ürge[3] and József Bakos[1]*

[1] *Department of Organic Chemistry, Institute of Environmental Engineering, University of Pannonia, H-8201 Veszprém, P. O. Box 158, Hungary*
[2] *Department of General and Analytical Chemistry, Budapest University of Technology and Economics, H-1111 Budapest, Szent Gellért tér 4, Hungary*
[3] *ThalesNano Nanotechnology Inc., 1031, Budapest, Záhony u. 7., Graphisoft Park, Hungary*

Highly active immobilized hydrogenation catalytic systems were used in the H-Cube™ hydrogenation reactor. "In situ" produced [Rh(COD)((*S*)-MonoPhos)$_2$]BF$_4$ complex was immobilized on commercially available Al_2O_3 and mesoporous Al_2O_3 by means of phosphotungstic acid (PTA), respectively. The optimum reaction conditions were determined and studied at different temperature, pressure, and flow rate values. Furthermore, the effect of the substrate concentration, microstructure of the support, and the stability of the complex were investigated. A continuous-flow reaction system using a stationary-phase catalyst for the asymmetric hydrogenation of methyl acetamidoacrylate was developed and run continuously for 12 h with >99% conversion and 96–97% enantioselectivity.

Keywords: asymmetric catalysis, continuous-flow system, heterogeneous catalysis, hydrogenation, supported catalysts, rhodium

1. Introduction

In the last several years, a worldwide renaissance in solid-state catalysis has been developed, driven by advances in materials science and growing environmental challenges. The immobilization of chiral catalysts for asymmetric reactions as one of the most promising solutions to the problem associated with the difficulties in the recovery and reuse of expensive homogeneous catalysts, as well as product contamination caused by the leaching, has attracted a great deal of interest recently. The a priori prediction of a suitable catalyst is still not obvious, and the experimental screening of catalyst is thus necessary. The vast majority of screening is usually performed in an autoclave, where the test of each catalytic system requires a new experiment with fresh substrate, catalyst, and solvent. Recent changes accelerated a growing demand in the pharmaceutical and fine chemical industry for a high-throughput continuous-flow reactor.

Monodentate phosphoramidites based on 1,1´-Bi-2-naphthol (BINOL) or substituted BINOL are excellent ligands for the rhodium-catalyzed asymmetric hydrogenations of olefins [1]. Very high enantioselectivities were obtained with MonoPhos, with the simplest member of this class. From an industrial point of view, however, solid catalysts that are not soluble in the same phase as the organic reactant have the inherent advantage of easy separation and, very often, also of better handling properties. Augustine and coworkers investigated different heteropolyanions (HPAs) as anchoring agents [2]. They found that the nature of the HPA can influence both the activity and the selectivity of the reactions. There is direct electrostatic interaction between the HPA and the metal atom of the active organometallic complex.

The [Rh(COD)((*S*)-MonoPhos)$_2$]BF$_4$ complex was successfully immobilized by Sheldon and coworkers on four different anionic carrier materials [3]: mesoporous aluminosilicate AlTUD-1, phosphotungstic acid (PTA) on alumina, Nafion, and Nafion silica composite [4]. The catalysts showed a virtually identical behavior to their homogeneous counterparts. Although most of the catalysts were highly selective, the activity and the loss of rhodium were strongly dependent on the type of support.

Besides, most studies on hydrogenation reactions are focused on using homogeneous catalysts that are difficult to separate from nonvolatile products and cannot be reused. The use of a microfluidics-based flow reactor (H-Cube) offers an elegant solution to both the problems mentioned above. It ensures a safe and easy manipulation of hydrogen of high pressure as well as the use of immobilized catalysts placed in CatCart® cartridges. Moreover, it enables the synthesis of chemical libraries of a great number of products in a short time and the optimization of reaction conditions in minutes.

Here, we report our results on the asymmetric hydrogenation of a benchmark substrate, such as methyl acetamidoacrylate, using immobilized [Rh(COD)((*S*)-MonoPhos)$_2$]$^+$ catalyst in the flow reactor [5]. A detailed investigation of the effects of changes in the reaction conditions (temperature, pressure, solvent, support, concentration of substrate, flow rate) has been carried out. The aim of this work is to demonstrate the use of supported HPAs, in the case of PTA, as carriers for chiral rhodium complexes, [Rh(COD)((*S*)-MonoPhos)$_2$]$^+$, and the efficient application of the immobilized catalyst in high-throughput microfluidics reactor.

2. Results and Discussion

2.1. Immobilization and Characterization of the Catalyst. The supports used in this work were commercially available neutral gamma-alumina and alumina produced in a special process indicated later, namely, mesoporous Al_2O_3. The overall mesoporosity of Al_2O_3, PTA/Al_2O_3, and [Rh(COD)(*S*)-(MonoPhos)$_2$]/PTA/Al_2O_3 was examined by nitrogen gas porosimetry, and the results are shown in Table 1 and Figure 1. It is important to note that for the clarity of the hysteresis curves (Figure 1), the measured adsorbed volumes of nitrogen were increased by values of 200 cm^3/g in the case of the samples of $Al_2O_3^{150}$ and $Al_2O_3^{401}$, and by values of 100 cm^3/g in the case of the samples of PTA/$Al_2O_3^{150}$ and PTA/$Al_2O_3^{401}$, respectively.

* Author for correspondence: bakos@almos.vein.hu

DOI: 10.1556/jfchem.2011.00002

Table 1. Textural information of supports and catalysts

Material	S_{BET} (m^2/g)	S_{BJH} (m^2/g)	S_{micro} (m^2/g)	$V_{1.7-300}$ (cm^3/g)	D_{av} (nm)
$Al_2O_3^{150}$	150.2	210.8	11.3	0.46	12.2
$PTA/Al_2O_3^{150}$	143.5	179.5	0	0.34	9.3
$[Rh(COD)((S)\text{-MonoPhos})_2]/PTA/Al_2O_3^{150}$	120.5	153.6	0	0.29	9.4
$Al_2O_3^{401}$	401.0	627.7	13.3	0.79	7.8
$PTA/Al_2O_3^{401}$	269.2	421.6	0	0.48	7.1
$[Rh(COD)((S)\text{-MonoPhos})_2]/PTA/Al_2O_3^{401}$	259.0	407.0	0	0.46	7.0

Table 2. Analytical data for $^1[Rh(COD)(S)\text{-}(MonoPhos)_2]/PTA/Al_2O_3^{150}$ and $^2[Rh(COD)(S)\text{-}(MonoPhos)_2]/PTA/Al_2O_3^{401}$ catalysts

Entry		Rh (m/m) (%)	P (m/m) (%)	W (m/m) (%)	P/Rh (mol-ratio)	Rh/PTA (mol-ratio)	P/PTA (mol-ratio)
1	Calculated	0.50	0.49	12.61	3	1	3
	Found	0.40	0.44	10.10	3.65	0.84	3.06
2	Calculated	0.43	0.43	12.27	3	1	3
	Found	0.30	0.31	10.15	3.50	0.63	2.20

The narrow pore-size distribution of the tested samples implies that the pores within the Al_2O_3 support and PTA/Al_2O_3 composites are uniform. Also, the Keggin units are homogeneously distributed across the condensed materials. It can be seen that Brunauer-Emmett-Teller (BET) surface areas and pore volumes of the PTA/Al_2O_3 and $[Rh(COD)((S)\text{-MonoPhos})_2]/PTA/Al_2O_3$ composites decreased with the PTA and catalyst loading. The average pore diameter of the composite is 9.4 nm, which is lower than the value measured for Al_2O_3 support. The pore diameter decreases from 12.9 to 9.4 nm, suggesting a partial blockage of the smaller pores of Al_2O_3 matrix by active species. The values of the pore volumes are 0.46, 0.32, and 0.29 cm^3/g, respectively. Similar to pure Al_2O_3, catalysts exhibited typical type-IV N_2 adsorption–desorption isotherms with H_1 hysteresis loop and visible step at P/P_0 = 0.50–0.80, corresponding to the capillary condensation of nitrogen in mesopores [6]. It must be outlined that while the commercial alumina ($Al_2O_3^{150}$) has adsorption ability of nearly 300 cm^3/g nitrogen Standard Temperature and Pressure (STP), the alumina produced in our process ($Al_2O_3^{401}$) can adsorb more than 500 cm^3/g nitrogen (STP). It can be inferred from the structural parameters shown in Table 1 that the incorporation of organometallic complexes onto both PTA and Al_2O_3 caused a decrease in mesopore size, surface area, and pore volume, obviously because of the coverage of pore surface with the organometallic complexes, leading to an increase in the original wall thickness and even partial blockage of the mesoporous channels [7]. Changing of the pore structure mentioned above is indicated in Figure 2 as well. The diameter values of the representative pores are smaller in the $Al_2O_3^{150}$ support produced by our method (about 5 nm instead of 9 nm), but there are many pores based on the value of frequency.

Table 2 lists the composition of anchored $[Rh(COD)((S)\text{-MonoPhos})_2]^+$ catalyst using this Keggin acid (PTA) as the anchoring agent. The elemental analysis Inductive Coupled Plasma (ICP) showed a Rh content of 0.40% (m/m) and a P

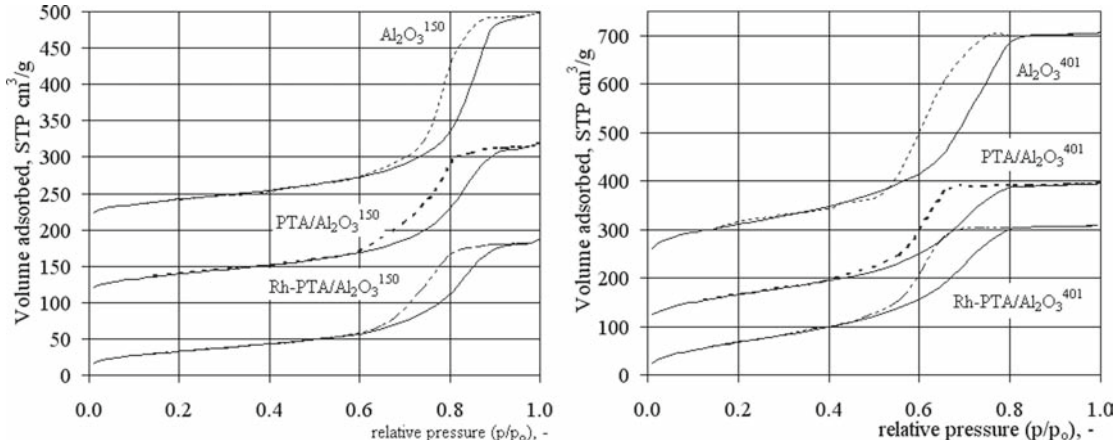

Figure 1. Nitrogen adsorption–desorption isotherms of supports and catalysts (Rh-PTA/Al_2O_3: $[Rh(COD)((S)\text{-MonoPhos})_2]/PTA/Al_2O_3$ catalyst, dotted line: desorption isotherm, continuous line: adsorption isotherm)

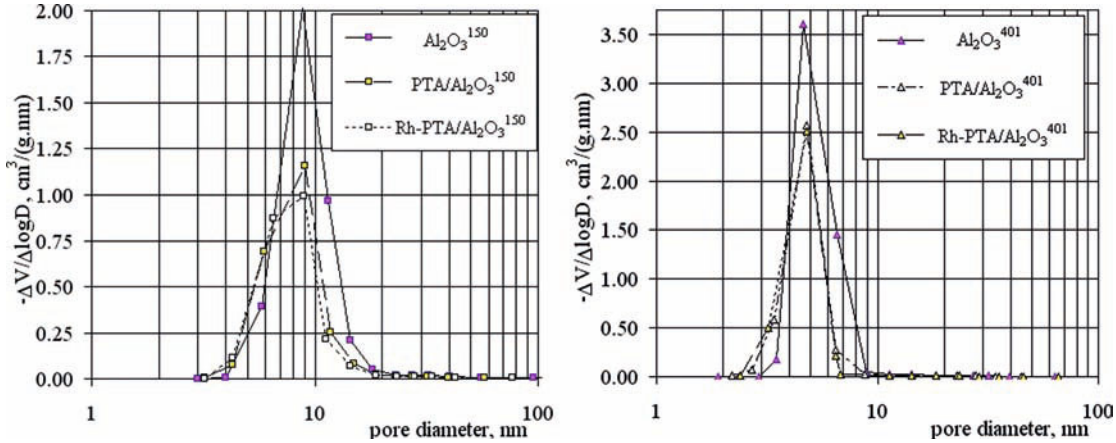

Figure 2. Pore volume frequency of supports and catalysts estimated by BJH method (Rh-PTA/Al_2O_3: $[Rh(COD)((S)\text{-MonoPhos})_2]/PTA/Al_2O_3$ catalyst)

content of 0.44%, whereas the theoretical contents were 0.50% and 0.49%, respectively. The color transfer from the rhodium complex solution to the white solid during the immobilization step showed a complete immobilization of the complex into the solid surface. For this step, the impregnation solvent of choice was anhydrous dichloromethane because of its aprotic and nonpolar nature and its capability to dissolve appreciable amount of the complex.

Structure integrity of the Keggin unit and Al_2O_3 support in the PTA/Al_2O_3 composites was studied by spectroscopic methods, including Fourier Transform Infrared (FT-IR) and ^{31}P Magic Angle Spinning (MAS) Nuclear Magnetic Resonance (NMR). A comparison of the FT-IR spectra of the parent PTA and PTA/Al_2O_3 composites shows that the characteristic vibrational frequencies related to the Keggin unit were unchanged for the tested PTA/Al_2O_3. These vibrational frequencies are 1079 (P—O central tetrahedral), 981 (terminal W═O), and 891 and 897 cm^{-1} (W—O—W), respectively, attributed to stretching vibrational modes of P—O, W═O, and W—O—W bonds of the Keggin unit [8]. However, the peak intensities decreased after the introduction of the Keggin unit into the Al_2O_3 framework.

^{31}P MAS NMR strongly supports the above results, with the characteristic P chemical shift (δ) of −18.7 ppm attributed to the PTA/$Al_2O_3{}^{150}$ composite (chemical shift is −15.5 ppm in the liquid phase). The chemical shift value is slightly different from the latter due to perturbations by the Al_2O_3 support.

The ^{31}P MAS NMR spectrum of [Rh(COD)((*S*)-MonoPhos)$_2$]/PTA/$Al_2O_3{}^{150}$ exhibits three signals: the peak at −18.3 ppm may originate from the PO_4 unit within $H_3PW_{12}O_{40}$ located near the Al_2O_3 surface without interaction with the rhodium complex. When the latter interaction exists, the signal shifts to lower field (+10.1 ppm). The third broad signal at 135.9 can be attributed to the ligand in the immobilized complex (δ 148.7 ppm for the free ligand and δ 130.8 ppm for [Rh(COD)((*S*)-MonoPhos)$_2$]BF_4 complex in the liquid phase).

2.2. Asymmetric Hydrogenation. The supported [Rh(COD)((*S*)-MonoPhos)$_2$]/PTA/$Al_2O_3{}^{150}$ catalysts were tested in the hydrogenation of methyl 2-acetamidoacrylate (MAA).

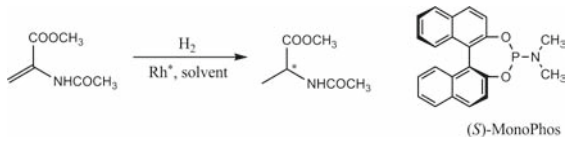

(*S*)-MonoPhos

Initially, the immobilized catalyst, [Rh(COD)((*S*)-MonoPhos)$_2$]/PTA/$Al_2O_3{}^{150}$, was packed into the CatCart® cartridges and used as the stationary heterogeneous catalyst phase. The effect of reaction parameters such as temperature, system pressure, flow rate, and substrate concentration (one cartridge was used for the evaluation of the effect of each parameter) was investigated in order to find the optimum conditions and a well-defined and reproducible catalytic system. The catalyst activity rapidly starts decreasing at about 50 °C (Table 3, entries 1–5), which can be attributed to leaching. Just a small decrease in the activity was observed from 20 to 40 °C. The fact that the Turnover Frequency (TOF) and the ee decrease, respectively, greatly and slightly at 60 °C can be explained by a faster and easier desorption of the catalyst at this condition.

The effect of the hydrogen pressure was also studied (entries 1, 6–8). The instrument works in two modes: when the reaction requires a larger amount of hydrogen, the option of full hydrogen mode is chosen, wherein large excess of hydrogen is generated at 1 bar (30 mL/min hydrogen vs. 0.1 mL/min solution, entries 1–5, 9–14) which gives a gas–liquid mixture. In this condition, the residence time in the reactor is extremely low (approximately 1 s at 0.1 mL/min flow rate) and at the same time the reactor operates with a H_2/S/Rh molar ratio of 240/1/360.

Table 3. Asymmetric hydrogenation of MAA in the flow reactor using [Rh(COD)((*S*)-MonoPhos)$_2$]/PTA/$Al_2O_3{}^{150}$ catalyst

Entry	T (°C)	c (M)	pH_2 (bar)	Q (mL/min)	Conv. (%)	ee (%)
1	20	0.05	1	0.1	96.4	96.9 (*R*)
2	30	0.05	1	0.1	85.5	95.8 (*R*)
3	40	0.05	1	0.1	83.3	96.3 (*R*)
4	50	0.05	1	0.1	77.9	96.1 (*R*)
5	60	0.05	1	0.1	28.0	93.6 (*R*)
6	20	0.05	10	0.1	92.0	96.2 (*R*)
7	20	0.05	20	0.1	>99	94.6 (*R*)
8	20	0.05	30	0.1	>99	93.2 (*R*)
9	20	0.05	1	0.2	50.3	97.7 (*R*)
10	20	0.05	1	0.3	41.7	96.7 (*R*)
11	20	0.05	1	0.4	34.5	95.8 (*R*)
12	20	0.2	1	0.1	77.1	95.6 (*R*)
13	20	1	1	0.1	54.2	93.6 (*R*)
14	20	3	1	0.1	36.1	92.9 (*R*)

Reaction conditions: solvent EtOAc, pressure drop on the CatCart: 1–2 bar. One cartridge was used for the evaluation of the effect of each parameter. The sample was taken under stationary conditions 40 min after the set of a new parameter. The total volume of the line is 3 mL.

In controlled (H_2) mode, the instrument gives a stable pressure level at the desired pressure. The hydrogen production is limited and the solubility of the hydrogen is dependent on pressure (*Henry's Law*). At higher pressures, a larger concentration of hydrogen will be present in the solution. The rate of bubbles in the liquid is regulated by a gas valve to keep a near-constant value of 7%, which means that the volume ratio of gas in the liquid phase at any time is independent of the applied pressure (entries 6–8). For example, at 10 bar of hydrogen the residence time in the reactor is around 2.5 min at 0.1 mL/min flow rate and at the same time the reactor operates with an approximate H_2/S/Rh molar ratio of 0.6/1/1.3.

It should be noted that the pressure at the outlet of the reactor was referring to the pressure of the hydrogen. The pressure drop on the CatCart® is about 1–2 bar. This means that the pressure in the gas/liquid mixer and at the inlet of the CatCart™ is 1–2 bar higher than that at the outlet. In general, up to 30 bar there was only a slight influence of the pressure on the selectivity. Higher pressure led to moderate drop of the enantioselectivity and almost quantitative conversion.

Higher flow rates resulted in lower conversions because of the shorter residence times of the reaction mixture in the reactor (entries 1, 9–11). On the other hand, with sufficiently small flow rates (e.g., 0.1 mL/min) high conversion could be achieved. The ee slightly decreased while the flow rates increased.

Importantly, the observed rate of the hydrogenation was found to be dependent on the substrate concentration, since the relative rate monotonously increased from a value of 21.8 to 489.4 h^{-1} on increasing the concentration from a value of 0.05 to the solubility limit (3.0 M) of the substrate in ethyl acetate (entries 1, 12–14).

On the basis of the experimental results compiled in Table 3, it can be concluded that [Rh(COD)((*S*)-MonoPhos)$_2$]/PTA/$Al_2O_3{}^{150}$ catalyst operates with the best efficiency at room temperature with low flow rate and substrate concentration.

As expected, the rhodium loss could largely be overcome by using less polar and aprotic solvent like ethyl acetate. In a continuous operation (entries 1–5); the reaction mixture was collected and the rhodium content of the solution was analyzed by ICP. The rhodium leaching could be reduced to 0.3 mg/L, which corresponds to 0.4% of the rhodium loading of the CatCart cartridge.

In order to prove that the reaction was heterogeneously catalyzed, and to exclude the possibility of homogeneous catalysis, the reaction mixture was separated from the catalyst before complete conversion occurred. The hydrogenation was continued under 10 bar of hydrogen for 2 h, and the reaction mixture

was analyzed to determine the conversion and enantioselectivity. No further reaction was observed (The conversion did not changes, remained 78.8%, and the enantioselectivity changed from 96.1%), whereas the original catalyst in the flow mode further hydrogenated the substrate. This test proved that no homogeneous catalysis took place.

The resulting heterogenized catalyst, [Rh(COD)((*S*)-MonoPhos)]/PTA/Al_2O_3[150], was also employed in the hydrogenation of MAA in a continuous-flow reactor (Table 4). Under the optimized experimental conditions (at 25 °C, under 1 bar of hydrogen pressure, with a flow rate of 0.1 mL/min and with a substrate concentration 0.05 M), the product could be obtained in a continuously decreasing conversion (95.5% to 74.4%) and in 95–97% enantioselectivity for a total of 8.5 h. This

Table 4. The stability of the catalysts in the hydrogenation of MAA in the flow reactor using [Rh(COD)((*S*)-MonoPhos)$_2$]/PTA/Al_2O_3[150]

Reaction time (min)	Conv. (%)	ee (%)
60	95.5	96.0 (*R*)
120	90.2	96.3 (*R*)
180	85.3	96.1 (*R*)
240	85.2	96.3 (*R*)
360	82.7	97.1 (*R*)
510	74.4	95.0 (*R*)

Reaction conditions: pressure of the hydrogen: 1 bar, solvent: EtOAc, reaction temperature: 25 °C, flow rate: 0.1 mL/min. Pressure drop on the CatCart: 3 bar, the concentration of the substrate: 0.05 M.

corresponds to a 0.036 g/h production of (*R*)-*N*-acetylalanine, giving an overall 0.3 g after 8.5 h.

To improve the productivity of the immobilized catalyst, the microstructure of the support was changed from Al_2O_3[150] to Al_2O_3[401]. As can be seen in Table 5, the hydrogenated product could still be obtained in almost quantitative yield with 97.7% ee after the 10th cycle, indicating that the catalyst does not lose a substantial amount of selectivity and activity upon recycling at an S/C ratio of 200. For this reaction, turnover number over 10 cycles is approximately 2000. This fact demonstrates that the stability of the catalyst can be enhanced by changing the microstructure of the support.

In order to prove that the reaction was heterogeneously catalyzed, and to exclude the possibility of homogeneous catalysis, filtration test was carried out [9]. After addition of the substrate to the supernatant of the fifth cycle, the hydrogenation was continued for 2 h. No further reaction was observed, whereas the original catalyst in the sixth cycle completely hydrogenated the substrate. This test proved that no homogeneous catalysis took place.

The data in Table 5 also show that practically no catalyst deactivation was observed so that further use of these catalysts was possible. These results demonstrate that modification of the microstructures of the support, namely, the anchored catalyst,

Table 5. The stability of the catalysts in the hydrogenation of MAA in batch mode using [Rh(COD)((*S*)-MonoPhos)$_2$]/PTA/Al_2O_3[401]

Run	Conv. (%)	ee (%)
1	>99.0	97.2 (*R*)
2	>99.0	97.6 (*R*)
3	>99.0	97.9 (*R*)
4	>99.0	97.6 (*R*)
5	>99.0	97.5 (*R*)
6	>99.0	97.6 (*R*)
7	>99.0	98.9 (*R*)
8	>99.0	98.4 (*R*)
9	>99.0	97.7 (*R*)
10	>99.0	97.6 (*R*)

Reaction conditions: pressure of the hydrogen: 5 bar, solvent: EtOAc, reaction temperature: 25 °C. 1 mmol of MAA was dissolved in 5 mL of EtOAc, S/Rh molar ratio: 200, reaction time: 30 min.

with larger support surface area exhibits higher stability (Table 3 vs. Table 5). It is interesting to note that in homogeneous asymmetric hydrogenation of MAA, quantitative conversion and 99.6% ee were observed [1]. The reaction was performed in EtOAc solvent at room temperature under ambient H_2 pressure for 20 h (substrate:[Rh(COD)$_2$]BF_4:ligand = 1:0.05:0.11).

The resulting heterogenized catalyst, [Rh(COD)((*S*)-MonoPhos)$_2$]/PTA/Al_2O_3[401], was also employed in the hydrogenation of MAA in a continuous-flow reactor (Table 6). Under the experimental conditions (at 25 °C, under 1 bar of hydrogen pressure, with a flow rate of 0.1 mL/min and with a substrate concentration 0.2 M), the product could be continuously obtained in >99% conversion and in 96–97% enantioselectivity for a total of 12 h. This corresponds to a 0.174 g/h production of (*R*)-*N*-acetylalanine, giving an overall 2.1 g after 12 h. It can be concluded that the immobilized catalyst, [Rh(COD)((*S*)-MonoPhos)$_2$]/PTA/Al_2O_3[401], is applicable in both batch recycling and continuous-flow process.

As a comparison, in a continuous-flow system using a well-designed self-supported chiral catalyst (MonoPhos derivative), a constant daily production of 0.36 g could be obtained in the asymmetric hydrogenation of methyl 2-acetamidocrotonate [10].

The performance of the catalyst seems to depend on the nature of support; higher activity and stability are observed with [Rh(COD)((*S*)-MonoPhos)$_2$]/PTA/Al_2O_3[401] than with [Rh(COD)((*S*)-MonoPhos)]/PTA/Al_2O_3[150] due to the larger surface area, pore volume and mesopore size of the support.

3. Conclusion

"*In situ*" produced [Rh(COD)((*S*)-MonoPhos)$_2$]BF_4 complex was immobilized on commercially available Al_2O_3 and mesoporous Al_2O_3 by means of PTA. In both cases, the incorporation of the PTA and the rhodium complex caused a decrease in the surface area, pore volume, and mesopore size of the support. A continuous-flow reaction system using a stationary-phase catalyst for the asymmetric hydrogenation of α-acetamidoacrylic acid methyl ester was developed and run continuously at 25 °C, under 1 bar of hydrogen pressure, with a flow rate of 0.1 mL/min and with a substrate concentration 0.2 M for 12 h with >99% conversion and 96–97% enantioselectivity. In this study, we have shown that anchored catalysts are suitable for flow reactors at temperature up to 60 °C. Furthermore, all hydrogenation results of supported catalysts indicate that supports with larger surface area exhibit higher stability.

4. Experimental

4.1. General Experimental Details. All manipulations were carried out under an atmosphere of argon using Schlenk techniques. Solvents were purified, dried, and deoxygenated

Table 6. The stability of the catalysts in the hydrogenation of MAA in the flow reactor using [Rh(COD)((*S*)-MonoPhos)$_2$]/PTA/Al_2O_3[401]

Reaction time (min)	Conv. (%)	ee (%)
0	>99	97.2 (*R*)
40	>99	97.1 (*R*)
160	>99	97.0 (*R*)
280	>99	96.9 (*R*)
340	>99	97.2 (*R*)
520	>99	96.6 (*R*)
580	>99	96.9 (*R*)
640	>99	97.1 (*R*)
700	>99	96.3 (*R*)
880	88.1	91.5 (*R*)
940	74.1	91.4 (*R*)
1060	63.3	91.6 (*R*)

Reaction conditions: pressure of the hydrogen: 1 bar, solvent: EtOAc, reaction temperature: 25 °C, flow rate: 0.1 mL/min. Pressure drop on the CatCart: 3 bar, the concentration of the substrate: 0.2 M.

by standard methods. All solvent transfers were carried out via cannula under positive argon pressure or by the use of gas-tight syringes. MonoPhos [11], $[Rh(COD)_2]BF_4$ [12], and α-acetamidoacrylic acid methyl ester [13] were prepared according to the literature procedure. The alumina used for the support was a neutral gamma-alumina obtained from Strem Chemicals and washed with ethanol to remove the fine particles before use. PTA was obtained from Merck. $^{31}P\{^1H\}$-, ^1H-NMR, and $^{13}C(^1H)$- spectra were recorded on either a VARIAN UNITY 300 spectrometer operating at 121.42, 300.15, and 75.43 MHz, respectively, or on a Bruker DRX-500 spectrometer operating at 202.45, 500.13, and 125.76 MHz, respectively. ICP elemental analyses were carried out using a GBC Integra XM (Australia) spectrometer.

The specific surface area and pore size distribution in the micropore (0–2 nm), mesopore (2–50 nm), and the macropore (50–300 nm) diameter ranges were determined by nitrogen adsorption/desorption isotherms measured with a Micromeritics ASAP 2000-type instrument on samples previously outgassed overnight in vacuum at room temperature. The surface areas of the samples (S_{BET}) were determined by the BET method from the corresponding nitrogen adsorption isotherm [14]. The meso- and macropore volume values were calculated from the nitrogen desorption isotherms using the BJH (Barret–Joyner–Halenda) theory [15].

The H-Cube® system is based on the hydrogenation of a continuous-flow of reactant. For the most basic function where only a continuous-flow of reactant is allowed through the system, only one High-Performance Liquid Chromatography (HPLC) pump is required [16]. Electrolytic water decomposition within the H-Cube® generates high-purity hydrogen in the required quantity, eliminating the need for gas storage. The hydrogen gas and a solution of the reactant are mixed, preheated, and transferred to a disposable catalyst cartridge (CatCart® that is preloaded with the required heterogeneous catalysts. The product then flows out of the cartridge and is collected in a vial or flask. The only workup required is the evaporation of solvent.

The continuous-flow of reaction mixture out of the device allows carrying out on-the-spot analysis of the resulting reaction mixture. Reaction parameters (*p*, *T*, flow rate/residence time) can be easily adjusted using a touch-screen interface in order to achieve a better product yield.

The CatCart® system is made up of a stainless steel tube packed with the heterogeneous catalyst of a specific particle size range (between 32–60 nm; CatCart® normal size: 30 × 4 mm). A filter system at either end of the tube allows liquid to pass through the column, but prevents catalyst from leaking out. Standard columns contain approximately 190 mg of catalyst with mesoporous Al_2O_3, and 390 mg of catalyst with commercially available Al_2O_3.

The dissolved substrate is mixed with the hydrogen gas in a gas–liquid mixer unit at the set pressure. The hydrogen–liquid mixture then passes through the cartridge preheated to the set temperature. The reaction takes place in the reactor zone before the product is pumped out. The product then flows out of the CatCart® into a collection vial.

4.2. Preparation of [Rh(COD)((S)-MonoPhos)$_2$]/ PTA/ Al_2O_3[150]. The PTA/Al_2O_3 was prepared by the slight modification of literature procedure [17]. The support obtained as a result was sieved, and the fraction with a particle size larger than 32 μm was used for the immobilization. Fifty-four grams of prewashed alumina was placed in a glass reactor and the system evacuated and re-filled with argon several times to remove the air from the pores of the solid. Four hundred and fifty milliliters of EtOH (95%) was added via cannula. A PTA solution (11.4 g in 150 mL EtOH) was added dropwise to the well-stirred alumina slurry via cannula. A stirrer was used to prevent grinding of the alumina between the magnetic stir bar and the bottom of the flask. After completion of the addition, the mixture was stirred for further 4 h. After this time, the reaction liquor was removed and the Al_2O_3/PTA was washed five times with 120 mL of ethanol. A solution of 264.4 mg of MonoPhos in 20 ml of CH_2Cl_2 was added to the solution of 145.7 mg of $[Rh(COD)_2]BF_4$ in 20 mL of CH_2Cl_2; then, it was stirred for 15 min. The solution of the in situ formed [Rh(COD)((*S*)-MonoPhos)$_2$]BF_4 complex was added to the well-stirred 7.0 g of Al_2O_3/PTA in 40 mL CH_2Cl_2 slurry dropwise via cannula. On completion, the mixture was stirred for 4 h, after which time the mixture was filtered. The product was then washed four times with 5 mL of CH_2Cl_2 and then the orange-yellow slurry was filtered and dried.

4.3. Preparation of PTA/Al_2O_3[401]. The mesoporous Al_2O_3 was prepared by the literature procedure [17]. The PTA/Al_2O_3 with mesoporous alumina was prepared by the slightly modified literature procedure. The resulting support was sieved, and the fraction with a particle size larger than 32 μm was used for immobilization.

4.4. Preparation of [Rh(COD)((S)-MonoPhos)$_2$]/PTA/ Al_2O_3[401]. The immobilized catalyst was prepared by the slightly modified literature procedure [6]. In situ formed [Rh(COD) ((*S*)-MonoPhos)$_2$]BF_4 was immobilized, and CH_2Cl_2 was used as the solvent.

4.5. Catalytic Hydrogenations in Batch Mode. A portion of anchored catalyst containing 5 μmol of the complex, 1.0 mmol of the substrate and 5 mL of EtOAc were placed in the stainless steel autoclave. The autoclave was purged with hydrogen gas and then pressurized to the appropriate initial pressure. The autoclave was stirred magnetically using a magnetic stirring bar for 30 min. At the end of the reaction, the stirring was stopped and the catalyst was allowed to settle and then the autoclave was depressurized. The reaction liquor was removed via cannula under a positive argon pressure and analyzed by Gas Chromatography (GC). The autoclave was then re-charged with 5 mL of EtOAc and a further portion of the substrate and the hydrogenation cycle was repeated.

4.6. Catalytic Hydrogenations in Flow Mode. The instrument works in two modes: when the reaction requires a larger amount of hydrogen, the option of full hydrogen mode is chosen. In this case, the H-Cube™ generates 30 mL/min hydrogen versus 0.1 mL/min flow rate of the solution at 1-bar pressure.

In the controlled (H_2) mode, the instrument gives one a stable pressure level at the desired pressure. The hydrogen production is limited, and the solubility of the hydrogen is dependent on pressure (*Henry's Law*). At higher pressures, a larger concentration of hydrogen will be present in the solution. The rate of bubbles in the liquid is regulated by a gas valve to keep a near-constant value of 7%, which means that a volume ratio of gas in the liquid phase at any time is independent of the applied pressure.

The anchored catalyst was filled into the CatCart in air. To ensure that all gases are removed from the reaction line, the system was washed with the solvent. The system was pressurized at 10 bar and the catalyst was prehydrogenated. The inlet tube was changed from the solvent to the reaction mixture and after 40 min a sample was taken, and the pressure was set at 1 bar. The reaction mixture was collected under inert gas atmosphere and the samples were analyzed on a Hewlett-Packard HP 4890 GC equipped with a split/splitless injector and a β-DEX 225 column (30 m, internal diameter 0.25 mm, film thickness 0.25 μm, carrier gas >99 kPa nitrogen, Flame Ionization Detector (FID) detector; the retention times of the two enantiomers are 7.1 min (*R*) and 7.9 min (*S*)).

Acknowledgments. The authors thank the National Office for Research and Technology (KMOP 1.1.4) for financial support. We thank Mr. Béla Édes for his skillful technical assistance.

5. References

1. (a) van der Berg, M.; Minnaard, A. J.; Schudde, E. P.; van Esch, J.; de Vries, A. H. M.; de Vries, J. G.; Feringa, B. L. *J. Am. Chem. Soc*. **2000**, *122*, 11539–11540. (b) van der Berg, M.; Minnaard, A. J.; Haak, R. M.; Leeman, M.; Schudde, E. P.; Meetsma, A.; Feringa, B. L.; de Vries, A. H. M.; Maljaars, C. E. P.; Willans, C. E.; Hyett, D.; Boogers, J. A. F.; Henderickx, H. J. W.; de Vries, J. G. *Adv. Synt. Catal*. **2003**, *345*, 308–323.
2. Augustine, R. L.; Tanielyan, S. K.; Mahata, N.; Gao, Y.; Zsigmond, A.; Yang H. *Appl. Catal. A* **2003**, *256*, 69–76.
3. Simons, C.; Hannefeld, U.; Arends, I. W. C. E.; Sheldon, R. A.; Maschmeyer, T. *Chem. Eur. J*. **2004**, *10*, 5829–5835.
4. (a) Simons, C.; Hannefeld, U.; Arends, I. W. C. E.; Minnaard, A. J.; Maschmeyer, T.; Sheldon, R. A. *Chem. Commun. J*. **2004**, 2830–2831. (b) Simons, C.; Hannefeld, U.; Arends, I. W. C. E.; Maschmeyer, T.; Sheldon, R. A. *J. Catal*. **2006**, *239*, 212–219.
5. For selected reviews on continuous flow reactors and processes, see (a) Kirsching, A.; Solodenko, W.; Mennecke, K. *Chem. Eur. J*. **2006**, *12*, 5972–5990. (b) Wiles, C.; Watts, P. *Eur. J. Org. Chem*. **2008**, 1655–1671. (c) Uozumi, Y.; Yamada, Y. M. A.; Beppu, T.; Fukuyama, N.; Ueno, M.; Kitamori, T. *J. Am. Chem. Soc*. **2006**, *128*, 15994–15995. (d) Smith, C. D.; Baxendale, I. R.; Lanners, S.; Hayward, J. J.; Smith, S. C.; Ley, S. V. *Org. Biomol. Chem*. **2007**, *5*, 1559–1561.
6. (a) Kruk, M.; Jaroniec, M.; Joo, S. H.; Ryoo, R. *J. Phys. Chem. B*. **2003**, *107*, 2205–2213. (b) Bao, X. Y.; Li, X.; Zhao, X. S. *J. Phys. Chem. B*. **2006**, *110*, 2656–2661.
7. (a) Liu, G. H.; Yao, M.; Zhang, F.; Gao, Y.; Li, H. X. *Chem. Commun*. **2008**, 347–349. (b) Liu, G. H.; Yao, M.; Wang, G. Y.; Liu, M. M.; Zhang, F.; Li, H. X. *Adv. Synth. Catal*. **2008**, *350*, 1464–1468.
8. Newman, A. D.; Lee, A. F.; Wilson, K.; Young, N. A. *Catal. Lett*. **2005**, *102*, 45–50.
9. Luan, Z. *Chem. Mater*. **1999**, *11*, 1621–1626.
10. Shi, L.; Wang, X.; Sandoval, C. A.; Wang, Z.; Li, H.; Wu, J.; Yu, L.; Ding, K. *Chem. Eur. J*. **2009**, *15*, 9855–9867.
11. Hulst, R.; de Vries, N. K.; Feringa, B. L. *Tetrahedron Asymmetry* **1994**, *5*, 699–708.
12. Schenk, T. G.; Downes, J. M.; Milne, C. R. C.; MacKenzie, P. B.; Boucher, T. G.; Whelan, J.; Bosnich, B. *Inorg. Chem*. **1985**, *24*, 2334.
13. Gladiali, S.; Pinna, L. *Tetrahedron Asymmetry* **1991**, *2*, 623–632.
14. Brunauer, S.; Emmett, P. H.; Teller, E. *J. Am. Chem. Soc*. **1938**, *60*, 309–319.
15. Barrett, P.; Joyner, L. G.; Halenda, P. P. *J. Am. Chem. Soc*. **1951**, *73*, 373–380.
16. http://thalesnano.com/Hcube
17. Shan, Z.; Jansen, J. C.; Zhou, W.; Maschmeyer, T. *Appl. Catal. A* **2003**, *254*, 339–343.